Does the isotropic–biaxial nematic transition always exist? A new topology for the biaxial nematic phase diagram

Gouripeddi Sai Preeti,[a,b] K.P.N. Murthy,[b] V.S.S. Sastry,[b] Cesare Chiccoli,[c] Paolo Pasini,[c] Roberto Berardi[a] and Claudio Zannoni*[a]

Received Xth XXXXXXXXXX 20XX, Accepted Xth XXXXXXXXX 20XX
First published on the web Xth XXXXXXXXXX 200X
DOI: 10.1039/b000000x

The biaxial nematic phase diagram for the second rank Straley quadrupolar pair potential, as explored until now, implies that a direct transition from a biaxial nematic to an isotropic phase can occur, either at a single Landau point or even, as recently shown using mean field theory, along a line. We show by an extensive Monte Carlo investigation that a different topology can be found in a wide region of parameter space, with the passage from biaxial to isotropic always going through a uniaxial phase. We argue that this may hint in part of the difficulty in realising a biaxial nematic phase.

1 Introduction

Biaxial nematic (N_b), fluids that possess two orthogonal preferred directions (directors) rather than the single one of standard nematics, have attracted considerable theoretical [1–7] and experimental [8–13] attention [14,15] ever since their existence was predicted over 30 years ago by Freiser [1] for a fluid of biaxial particles interacting with a quadrupolar like potential. As real mesogenic molecules are non cylindrically symmetric, it would seem natural to expect to find this lower symmetry biaxial nematic phase as well as the standard uniaxial (N_u) one. On the contrary the existence of the phase has been demonstrated in lyotropics [16] and in polymer liquid crystals [17,18], but has proved to be extremely elusive on low molar mass thermotropics and has defied experimental attempts at preparing it either in pure mesogens or mixtures [19–21] (see [22] for a recent review) until recently, when its observation in bow shaped mesogens [8,9,13], and other families of compounds [10,12], has immediately given rise to a burst of theoretical and experimental activity in a variety of materials [11,22–24]. The reasons for this interest are both of fundamental and technological nature. The first and more profound is the challenge to understand why a phase that was predicted by Mean Field (MF) theory [1,25], computer simulations of lattice [26,27], off–lattice models of the hard–repulsive [28] and of the attractive–repulsive kind [29] in pure mesogens, and recently in mixtures of uniaxial rods and discs [30], is so difficult to realize in practice. The second deals with the prospect of novel and faster electro-optical devices that can be obtained through a control of the secondary director axis [31]. The two aspects are strictly correlated, given that the current biaxial nematics are hardly suitable for practical applications because of their material features (high transition temperatures, viscosities etc.) and because attempts at tweaking the molecular structure [32] are likely to fail in the absence of at least a general knowledge of the phase diagram.

The layout of the paper is the following: after this *Introduction*, a *Modelling* Section describes the biaxial pair potential used to compute the energy between neighbouring spins in a cubic lattice; the *Monte Carlo simulations* gives the technical details of our calculations; the *Results and discussion* Section provides the outcomes of the Monte Carlo simulations and in particular the phase diagram; the *Conclusions* Section summarises the results.

2 Modelling

Here we wish to provide the general phase diagram mentioned in the Introduction and we start from the most general purely orientational pair potential between two rigid particles with biaxial D_{2h} symmetry, that has been put forward by Straley [2] and recently revisited, see e.g. [3,33]. This can be obtained in a general way as a result of averaging the full pair potential, dependent on the intermolecular vector $\mathbf{r}_{ij}$ and on the position–orientations of the two particles, r_i, ω_i, r_j, ω_j, over the distribution of $\mathbf{r}_{ij}$ [26,34]. For a cubic lattice with nearest neighbor interactions, as assumed here, the average gives

[a] *Dipartimento di Chimica Fisica e Inorganica, Università di Bologna, Bologna, Italy, Fax: +39 051 2093690; Tel: +39 051 2097012; E–mail: claudio.zannoni@unibo.it*
[b] *School of Physics, University of Hyderabad, Hyderabad, India.*
[c] *Istituto Nazionale di Fisica Nucleare, Sezione di Bologna, Bologna, Italy*

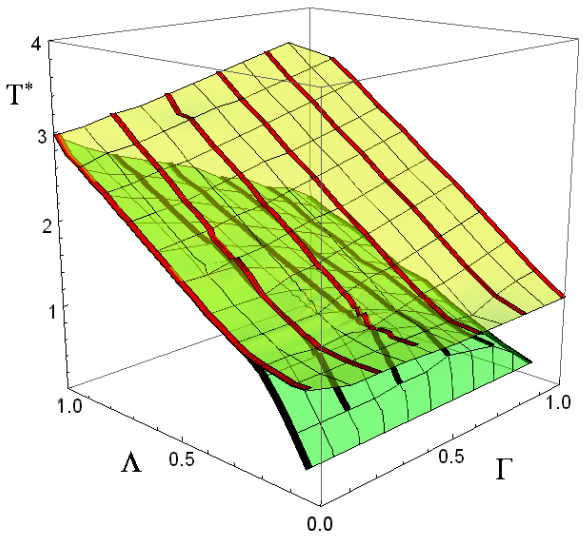

Fig. 1 Phase diagram of the order–disorder transition: reduced temperatures T^* versus the biaxial parameters Γ, and Λ of Eq. 3 as obtained from MC simulations on a $20 \times 20 \times 20$ lattice. The two surfaces denote the transitions from an isotropic (I) to uniaxial nematic (N_u) phase (pale yellow surface, with superimposed red lines), and from N_u to biaxial nematic (N_b) (pale green surface, with superimposed black lines). The T^* points at constant Γ values have been interpolated and the resulting two sets of red and black lines have been plotted as guides to the eye for a better appreciation of the N_u gap separating the N_b and I phases at high Γ values (see text).

$$\begin{aligned} U_{ij} =& u_{200} R^2_{0,0}(\cos\beta_{ij}) \\ &+2u_{220}[R^2_{0,2}(\omega_{ij}) + R^2_{2,0}(\omega_{ij})] \\ &+4u_{222} R^2_{2,2}(\omega_{ij}), \end{aligned} \tag{1}$$

where $R^2_{m,n}$ are functions obtained by applying the D_{2h} projection operator to the $D^{L\,*}_{m,n}$ Wigner matrices

$$\begin{aligned} R^L_{m,n} =& \frac{1}{4}\delta_{L,\mathrm{even}}\delta_{m,\mathrm{even}}\delta_{n,\mathrm{even}} \\ &\times \left(D^{L\,*}_{m,n} + D^{L\,*}_{m,-n} + D^{L\,*}_{-m,n} + D^{L\,*}_{-m.-n}\right). \end{aligned} \tag{2}$$

The $R^2_{m,n}$ are functions of the relative rotation angles from i to j[35], i.e. $\omega_{ij} \equiv (\alpha_{ij}, \beta_{ij}, \gamma_{ij})$,[27]. The model reduces to the well known uniaxial Lebwohl–Lasher potential[36–38] when $u_{220} = u_{222} = 0$. In the notation introduced by Romano[39], as well as Virga and coworkers[40], that we shall use in what follows, the previous equation becomes

$$\begin{aligned} U_{ij} = \varepsilon \{ &-G_{33} + \Gamma\,(G_{11} - G_{22}) \\ &-\Lambda\,[2(G_{11} + G_{22}) - G_{33}]\}, \end{aligned} \tag{3}$$

where $G_{mn} \equiv P_2(\mathbf{u}^i_m \cdot \mathbf{u}^j_n)$ and $\mathbf{u}^i_m$, with $m = 1, 2, 3$, is the triplet of orthogonal unit vectors representing the axis system of particle i. By comparison $\varepsilon = -u_{200}$, $\Gamma = \sqrt{(8/3)}(u_{220}/u_{200})$, and $\Lambda = (2/3)(u_{222}/u_{200})$. We notice that the potential in Eq. 1 can be considered as the second rank contribution in a more general expansion over Wigner rotation matrices of rank L. As such the coefficients u_{2mn}, and consequently Γ, Λ, do not have a simple physical identification in terms of single molecule properties, as it would be desirable. In general, since u_{200} can be used to define a reduced temperature $T^* \equiv -k_B T/u_{200}$, the potential in Eq. 3 depends on the parameters Γ, Λ that define a two dimensional space.

There are however a few cases studied, e.g. when dispersion interactions are assumed and an average over intermolecular separations is performed[26], in which the interaction coefficients could be written as $u_{2mn} = k_{ij}\alpha^{2m}\alpha^{2n}$, where α^{2p} are the spherical components of the molecular polarizability tensor and k_{ij} a constant[26], so that $u_{222}/u_{200} = (u_{220}/u_{200})^2$ or $\Lambda = \Gamma^2/4$. This special case has been widely studied by Monte Carlo (MC) simulations[27,41,42] and for this Hamiltonian, even if MF overestimates the transition temperatures, the topology of the phase diagrams obtained from MC simulations and MF models is the same, with a Landau point where a direct transition from N_b to isotropic (I) phase takes place. Simple models based on excluded volume or on an interaction proportional to the exposed surface in different directions, that allow to work out Γ, Λ from the length L, breadth B, width W of brick–like molecules have been put forward by Straley[2] and by Ferrarini *et al.*[43] and correspond to a subspace of (Γ, Λ) space. A phase diagram was obtained for a specific choice of parameters, i.e. $\Gamma = 0$[3]. Virga, Romano and coworkers showed that in this case a coexistence line between N_b and I phases is obtained, and these findings were confirmed by MC at selected state points[39,40,44]. For this subset of parameters a biaxial phase should be the first one observed on cooling down from the isotropic, hence it should be relatively easy to find, contrary to experimental evidence.

More recently, Virga and coworkers[5,40] have analyzed the general Hamiltonian in Eq. 3. They have shown that the potential yields a stable minimum for calamitic states (parallel side by side blocks) only within a certain fan–shaped region of parameter space defined by $\Lambda - |\Gamma| + 1 > 0$. However, the key questions of topology of the phase diagram and of the sequence in which the various phases occur on cooling from the isotropic are still unanswered. The aim of the present letter is thus to present a detailed MC investigation[45] of the general Straley biaxial Hamiltonian Eq. 3[2,3,33] and to obtain its phase diagram.

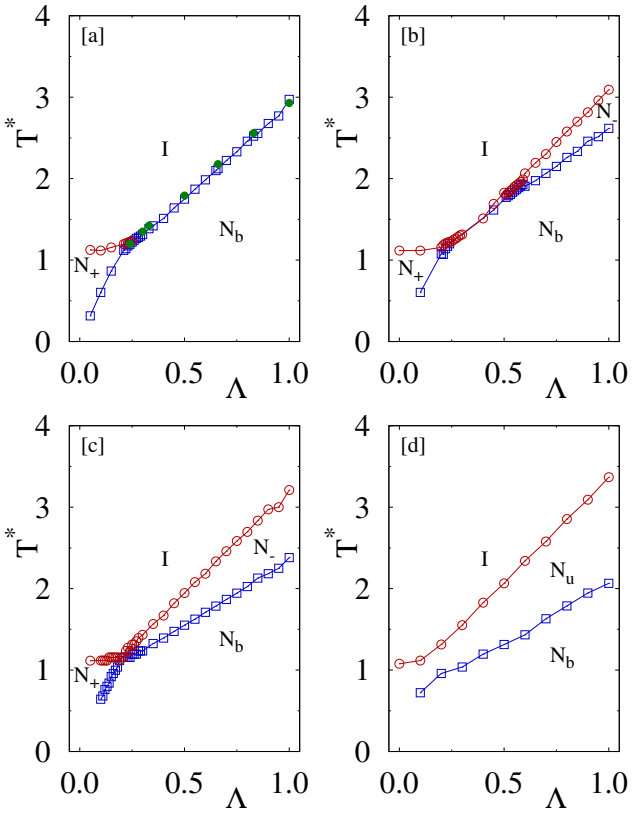

Fig. 2 Sections of the biaxial phase diagram for $\Gamma = 0$ (plate [a]), 0.2 (plate [b]), $0.4 \approx 1/\sqrt{6}$ (plate [c]), and 0.6 (plate [d]) values of the phase diagram of Fig. 1 giving the transition temperatures T^* as a function of the Λ parameter of Eq. 3. The green points in plate [a] with $\Gamma = 0$ have been taken from Refs.[40,44]

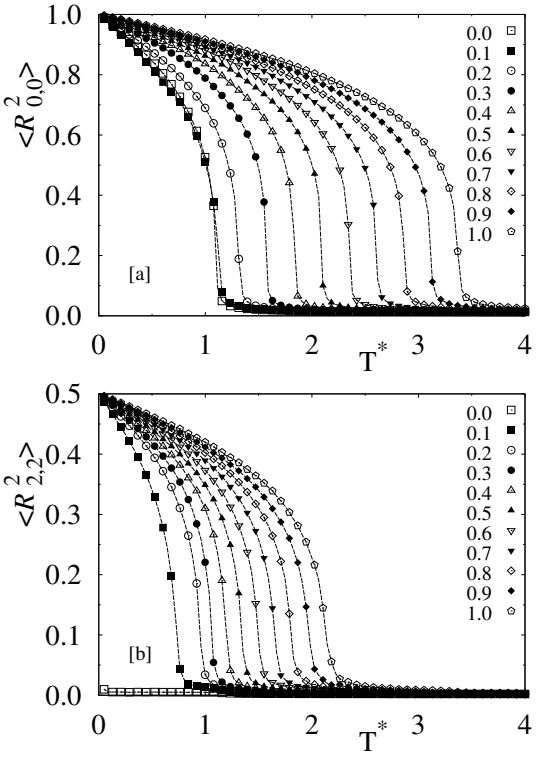

Fig. 3 Temperature dependence of the average $\langle R^2_{0,0} \rangle$ (plate [a]) and $\langle R^2_{2,2} \rangle$ (plate [b]) order parameters from MC simulations at the indicated Λ values and constant $\Gamma = 0.6$. Symbols have been drawn every two MC data points

3 Monte Carlo simulations

We have considered a $20 \times 20 \times 20$ simple cubic lattice with periodic boundary conditions of biaxial particles interacting through the nearest neighbor version of the potential in Eq. 3 and performed MC simulations over a 10×10 regularly spaced grid of (Γ_i, Λ_j) values, with $0 \leq \Gamma_i \leq 1$, $\Delta\Gamma = 0.1$ and $0 \leq \Lambda_j \leq 1$, $\Delta\Lambda = 0.1$. Simulations have been started from random particle orientations at dimensionless temperature $T^* = 4$ and, for every (Γ_i, Λ_j) pair, a sequence of 100 temperature cooling–down scans was performed until the final $T^* = 0.04$ was attained. Orientations were updated choosing one of the three axis at random and using the Barker–Watts[46] method on each attempted Monte Carlo move. Every sample was first equilibrated for $250,000$ MC sweeps starting from the final configuration of the previous temperature point, then equilibrium averages have been computed over at least $250,000$ additional MC sweeps. Besides the relevant thermodynamic observables (*e.g.* average potential energy, and specific heat), we have computed a full set of second rank order parameters $\langle R^2_{0,0} \rangle$, $\langle R^2_{2,0} \rangle$, $\langle R^2_{0,2} \rangle$, and $\langle R^2_{2,2} \rangle$, i.e. S, $\sqrt{3/2}T$, $S'/\sqrt{6}$, $T'/2$[47] or S, $P/\sqrt{2}$, $U/\sqrt{2}$, $F/2$[48] using the algorithm outlined in Refs.[27,42].

The transition temperatures T^* have been estimated from the position of the maxima in the specific heat capacity obtained in turn from mean square energy fluctuations.

4 Results and discussion

Our main result is the overall phase diagram presented in Fig. 1 where the two surfaces enveloping the transition temperatures T^* from I to N_u, and from N_u to N_b respectively are represented with superimposed thick lines as guides for the eye. In addition, to highlight the most relevant features of this phase diagram four sections at constant $\Gamma = 0$, 0.2, 0.4, and 0.6 values are shown in Fig. 2. The plots of Figs. 1–2 reveal that for the smaller values of Γ there is a wide Λ range where, upon cooling, the system goes directly from isotropic to biaxial nematic phase (see Fig. 2–(a)). In particular, for the case $\Gamma = 0$, we confirm the findings of Romano[39] of a triple point

at $\Lambda = 0.26$, and a line of I–N_b transitions up to $\Lambda = 1$. As Γ increases the triple point at $\Lambda = 0.26$ gradually shifts towards lower values. This corresponds to the appearance of a second triple point which regularly shifts downwards from the initial $\Lambda = 1$ value for $\Gamma = 0$ (see Fig. 2–[b]) as Γ increases. The line through the triple points connects two wedge–shaped regions of uniaxial *"calamitic nematic"* (*so–called* N_+), obtained in the dispersive model for $0 \leq \Lambda < 1/\sqrt{6}$, and *"discotic nematic"* (*so–called* N_-), obtained in the dispersive model for $1/\sqrt{6} < \Lambda \leq 1$, phases bracketing a central Λ range characterized by direct I–N_b transition.

All systems with $\Lambda = 0$ have been found to form only uniaxial nematics. Conversely, N_b is always observed whenever $\Lambda > 0$. This behavior originates from the role Λ has in Eq. 3 influencing the weight of the terms coupling the orientations of the transversal axes (and thus phase biaxiality).

For $\Gamma \approx 0.4$ the connecting line shrinks to essentially a point, similarly to the dispersive case[27]. For $\Gamma > 0.4$ the two phase boundary lines depart and a direct transition from I to N_b phase is no longer possible. More in detail we see from Figs. 1–2 that the effect of increasing Γ (at constant Λ) is that of lowering T_{N_b}. So, if we take $\Gamma = 0.4 \approx 1/\sqrt{6}$ as a reference, an increase of Γ results in stabilizing N_u and destabilizing N_b, while any molecular interaction mechanism giving $\Gamma < 0.4$ should provide a substantial increase of the temperature stability for the N_b phase.

The location of the transitions is also supported by the temperatures variations of the most relevant order parameters[27] $\langle R^2_{0,0}\rangle$ and $\langle R^2_{2,2}\rangle$ plotted in Fig. 3. In particular, $\langle R^2_{0,0}\rangle$ and $\langle R^2_{2,2}\rangle$ are both non zero in the N_b phase, while in the uniaxial nematic phase only $\langle R^2_{0,0}\rangle > 0$ while $\langle R^2_{2,2}\rangle < 0.05$. In the isotropic phase both order parameters vanish.

We observe that in our exploration of the biaxial phase diagram we have not found instances of order parameters with magnitude in the unusual sequence previously reported[10], thus confirming also for this study the earlier results[5].

In real, or at least off–lattice, systems biaxial nematic competes for existence with smectic and crystalline phases[29], which are typically estimated to take place in a temperature range of some 10% from the isotropic transition temperature[43]. Thus emergence of nematic phase biaxiality is much more difficult in practice than what is predicted by lattice models and has to take place in a rather narrow temperature range below the transition to isotropic phase. As a consequence, as we see from Fig. 2 for large Γ a biaxial nematic not contiguous to the isotropic, but instead lying well below the uniaxial phase is unlikely to be observed. This can be connected with the fact that upon increasing Γ there is a change in the pair potential in Eq. 3 from maximum to minimum around the point where the angles α_{ij}, β_{ij} between the x and the z axes respectively of the two molecules are $\alpha_{ij} = 0°$, $\beta_{ij} = 90°$. Then it becomes a saddle point, indicating that for high Γ the *face–to–face* configuration is relatively destabilized when the two molecules happen to be nearly perpendicular, a situation more likely to arise when the system is close to being isotropic phase.

5 Conclusions

In summary, we have shown that over a wide range of parameters the molecular organization obtained on cooling from the isotropic is a uniaxial nematic, while the biaxial phase is confined to low temperatures where realistic systems probably would become smectic or crystals. This is a rather more pessimistic view than that provided by the extended isotropic–biaxial nematic transition line found in[39,40,44], but one which seems consistent with the persistent difficulty in finding biaxial nematics. Even though our results are based on a simple model dealing only with orientational properties we believe the topology of the phase diagram should be quite general and useful for comparing and understanding the results of real experiments. This has proved true in the past for even simpler purely orientational models[3,27] used by experimentalists (see *e.g.*[10,32]). Going from general consideration to specific cases, it is worth remarking that it is not easy instead to establish a simple connection between the potential parameters u_{2mn} and molecular properties since, in general the second rank part of the potential is just a term in the expansion of a realistic potential. Even the simple repulsive, surface or dispersive interactions already mentioned[2,27,43] can operate and contribute concurrently to the second rank potential. Indeed a combination of biaxial attractive and repulsive interactions of opposite sign was found important in obtaining biaxial nematic phases of generalized Gay-Berne mesogens[29]. A connection between molecular structures and potential coefficients can however be established, as recently shown by Gorkunov *et al.*[49] for molecules as complex as biaxial tetrapods[10,12], starting from a detailed molecular potential with a certain physical origin and expanding it in a multipolar series, that is then truncated at rank $L = 2$. Using a slightly different formulation from[49], *i.e.* assigning an approximate pair distribution $\exp[-U^{GB}_{ij}(r_{ij},\omega_1,\omega_2,\omega_r)/\epsilon_0]$ (implicitly at unit temperature since we are mostly interested in the trend of the expansion coefficients), we can write $u_{Lmn}(r_{ij})$ as

$$u_{Lmn}(r_{ij}) = \frac{1}{C}\int R^L_{m,n}(\omega_2) U^{GB}_{ij}(r_{ij},\omega_1,\omega_2,\omega_r) \times e^{-U^{GB}/\epsilon_0} d\omega_2\, d\omega_r, \quad (4)$$

where $C = 32\pi^3$ is the normalisation factor. Instead of integrating with respect to the particle–particle $\omega_{12} = (\alpha_{12},\beta_{12},\gamma_{12})$, we have placed the first molecule in the reference frame centre with fixed $\omega_1 = (0,0,0)$ orientation, and

allowed the second particle to span all remaining orientational degrees of freedom $\omega_2 = (\alpha_2, \beta_2, \gamma_2)$, and $\omega_r = (\alpha_r, \beta_r)$. The integrals have been evaluated using a five–dimensional gridding of the entire ω_2, ω_r domain using 32 evenly spaced points for each variable (test calculations using 64^5 evenly spaced points confirm these values). In particular, we have used three approaches for the computation of the integrals: (a) all U^{GB} values larger than $10\ \epsilon_0$ have been flattened, *i.e.* $U^{GB} = \min[U^{GB}, 10\ \epsilon_0]$; (b) all $U^{GB} \geq 10\ \epsilon_0$ points have been set to $0\ \epsilon_0$; (c) all $U^{GB} \geq 0\ \epsilon_0$ have been set to $0\ \epsilon_0$ as in reference[49]. The three approaches for dealing with the positive branch of the U^{GB} surface practically give the same results. Notice that while this procedure allows to obtain Straley coefficients Γ, Λ from a biaxial GB potential, the inverse problem of finding a GB parameterisation from Γ, Λ is clearly undetermined.

For instance, in the case of the biaxial Gay-Berne potential[50,51] with the parameterization that has been shown to lead to a biaxial nematic[29,31] the second rank expansion coefficients obtained with this procedure, assuming $r_{ij} > r_s$, where r_s is of the order of a molecular length give $\Gamma \approx 0.092$, $\Lambda \approx 0.24$. It is interesting to see that in this case the simulations show the phase sequence isotropic, uniaxial nematic, biaxial nematic as expected from the phase diagram in Fig. 1. Even though computer simulations need to be used for a definite prediction, we believe that this type of approach might help in the rational design[32] of real biaxial mesogens, identifying favourable parameter ranges leading to the desired region of the general phase diagram reported here.

Acknowledgments

We wish to acknowledge the EU–STREP project *"Biaxial Nematic Devices"* (BIND) FP7–216025 and the Department of Science and Technology (HPCF), India (UH/CMSD/HPCF/2006–2009) for financial support and the Center for Modelling, Simulation and Design, University of Hyderabad for its facilities.

References

1 M. J. Freiser, *Phys. Rev. Lett.*, 1970, **24**, 1041–1043.
2 J. P. Straley, *Phys. Rev. A*, 1974, **10**, 1881–1887.
3 A. M. Sonnet, E. G. Virga and G. E. Durand, *Phys. Rev. E*, 2003, **67**, 061701.1–7.
4 F. Bisi, E. G. Virga, E. C. Gartland, G. De Matteis, A. M. Sonnet and G. E. Durand, *Phys. Rev. E*, 2006, **73**, 051709.
5 F. Bisi, G. R. Luckhurst and E. G. Virga, *Phys. Rev. E*, 2008, **78**, 021710–1.6.
6 S. Varga, A. Galindo and G. Jackson, *Phys. Rev. E*, 2002, **66**, 011707–16.
7 R. Berardi, L. Muccioli, S. Orlandi, M. Ricci and C. Zannoni, *J. Phys.: Condens. Matter*, 2008, **20**, 463101–16.
8 L. A. Madsen, T. J. Dingemans, M. Nakata and E. T. Samulski, *Phys. Rev. Lett.*, 2004, **92**, 145505.1–4.
9 B. R. Acharya, A. Primak and S. Kumar, *Phys. Rev. Lett.*, 2004, **92**, 145506.1–4.
10 K. Merkel, A. Kocot, J. K. Vij, R. Korlacki, G. H. Mehl and T. Meyer, *Phys. Rev. Lett.*, 2004, **93**, 237801.1–4.
11 K. Severing and K. Saalwachter, *Phys. Rev. Lett.*, 2004, **92**, 125501.
12 J. L. Figueirinhas, C. Cruz, D. Filip, G. Feio, A. C. Ribeiro, Y. Frère, T. Meyer and G. H. Mehl, *Phys. Rev. Lett.*, 2005, **94**, 107802.1–4.
13 Y. Jang, V. Panov, A. Kocot, J. Vij, A. Lehmann and C. Tschierske, *Appl. Phys. Lett.*, 2009, **95**, 183304.
14 G. R. Luckhurst, *Thin Solid Films*, 2001, **393**, 40–52.
15 G. R. Luckhurst, *Nature*, 2004, **430**, 413–414.
16 L. J. Yu and A. Saupe, *Phys. Rev. Lett.*, 1980, **45**, 1000–1003.
17 F. Hessel and H. Finkelmann, *Polymer Bulletin*, 1986, **15**, 349–352.
18 K. Severing and K. Saalwächter, *Phys. Rev. Lett.*, 2004, **92**, 125501.
19 R. Pratibha and N. V. Madhusudana, *Mol. Cryst. Liq. Cryst. Letters*, 1985, **1**, 111–116.
20 J. J. Hunt, R. W. Date, B. A. Timimi, G. R. Luckhurst and D. W. Bruce, *J. Am. Chem. Soc.*, 2001, **123**, 10115–10116.
21 R. W. Date and D. W. Bruce, *J. Am. Chem. Soc.*, 2003, **125**, 9012–9013.
22 C. Tschierske and D. Photinos, *J. Mater. Chem.*, 2010, **20**, 4263–4294.
23 E. van den Pol, A. V. Petukhov, D. M. E. Thies-Weesie, D. V. Byelov and G. J. Vroege, *Phys. Rev. Lett.*, 2009, **103**, 258301.
24 M. Nagaraj, Y. Panarin, U. Manna, J. Vij, C. Keith and C. Tschierske, *Appl. Phys. Lett.*, 2010, **96**,.
25 M. J. Freiser, *Mol. Cryst. Liq. Cryst.*, 1971, **14**, 165–182.
26 G. R. Luckhurst, C. Zannoni, P. L. Nordio and U. Segre, *Mol. Phys.*, 1975, **30**, 1345–1358.
27 F. Biscarini, C. Chiccoli, P. Pasini, F. Semeria and C. Zannoni, *Phys. Rev. Lett.*, 1995, **75**, 1803–1806.
28 M. P. Allen, *Liq. Cryst.*, 1990, **8**, 499–511.
29 R. Berardi and C. Zannoni, *J. Chem. Phys.*, 2000, **113**, 5971–5979.
30 A. Cuetos, A. Galindo and G. Jackson, *Phys. Rev. Lett.*, 2008, **101**, 237802.1–4.
31 R. Berardi, L. Muccioli and C. Zannoni, *J. Chem. Phys.*, 2008, **128**, 024905.1–12.
32 D. W. Bruce, *The Chemical Record*, 2004, **4**, 10–22.
33 G. De Matteis and S. Romano, *Phys. Rev. E*, 2009, **80**,

031702.
34 G. R. Luckhurst, *Liq. Cryst.*, 2009, **36**, 1295–1308.
35 M. Rose, *Elementary Theory of Angular Momentum*, Wiley, 1957.
36 P. A. Lebwohl and G. Lasher, *Phys. Rev. A*, 1972, **6**, 426–429.
37 P. A. Lebwohl and G. Lasher, *Phys. Rev. A*, 1973, **7**, 2222.
38 U. Fabbri and C. Zannoni, *Mol. Phys.*, 1986, **58**, 763–788.
39 S. Romano, *Physica A*, 2004, **337**, 505–519.
40 G. D. Matteis, S. Romano and E. G. Virga, *Phys. Rev. E*, 2005, **72**, 041706.1–13.
41 G. R. Luckhurst and S. Romano, *Mol. Phys.*, 1980, **40**, 129.
42 C. Chiccoli, P. Pasini, F. Semeria and C. Zannoni, *Int. J. Mod. Phys. C*, 1999, **10**, 469–476.
43 A. Ferrarini, P. Nordio, E. Spolaore and G. Luckhurst, *J. Chem. Soc. Faraday Trans.*, 1995, **91**, 3177–3183.
44 S. Romano, *Phys. Lett. A*, 2004, **333**, 110–119.
45 P. Pasini and C. Zannoni, *Advances in the Computer Simulations of Liquid Crystals*, Kluwer, 2000.
46 J. A. Barker and R. O. Watts, *Chem. Phys. Lett.*, 1969, **3**, 144–145.
47 F. Bisi, S. Romano and E. G. Virga, *Phys. Rev. E*, 2007, **75**, 041705.
48 R. Rosso, *Liq. Cryst.*, 2007, **34**, 737–748.
49 M. V. Gorkunov, M. A. Osipov, A. Kocot and J. K. Vij, *Phys. Rev. E*, 2010, **81**, 061702.1–10.
50 R. Berardi, C. Fava and C. Zannoni, *Chem. Phys. Lett.*, 1995, **236**, 462–468.
51 R. Berardi, C. Fava and C. Zannoni, *Chem. Phys. Lett.*, 1998, **297**, 8–14.